SCARAB - A MULTI-DISCIPLINARY CODE FOR DESTRUCTION ANALYSIS OF SPACE-CRAFT DURING RE-ENTRY

Georg Koppenwallner[(1)], Bent Fritsche[(2)], Tobias Lips[(3)], Heiner Klinkrad[(4)]

[(1)] HTG, D-37191 Katlenburg Lindau, Max Planck Strasse 19; G.Koppenwallner@HTG-HST.de
[(2)] HTG, D-37191 Katlenburg Lindau, Max Planck Strasse 19; B.Fritsche@HTG-HST.de
[(3)] HTG, D-37191 Katlenburg Lindau, Max Planck Strasse 19; T.Lips@HTG-HST.de
[(4)] ESOC, D-64293 Darmstadt, Robert Bosch Strasse 5; Heiner.Klinkrad@ESA.int

Abstract

The uncontrolled, destructive re-entry of satellites and the related ground risk due to fragments reaching the ground have become of increased interest during the past years. The software system SCARAB (Spacecraft Atmospheric Re-entry and Aerothermal Break-up) is designed to calculate the destruction of a spacecraft during re-entry. Development of this code system started in 1995 and was conducted by HTG within the frame of various ESOC contracts with ITAM in Novosibirsk as continuous partner.
The modular software system provide modules for satellite modelling and re-entry analysis The analysis modules combine aerodynamic/aero-thermal loads, 6-D flight dynamic, heat conduction, destruction by melting or fracture and the fragment tracking till ground impact
SCARAB has been applied to many projects like ARIANE 5, ATV, ROSAT, Beppo SAX and Terrasar.

1. Introduction

The SCARAB simulation software is an integrated system combining spacecraft modelling modules and the analysis modules for the destructive re-entry [1], [2], [3]. Special demands on the code resulted directly from the field of application.

- Re-entry uncontrolled with tumbling motion
- Shape of spacecraft may be very complex
- Internal structure must be considered
- Shape is not based on aerodynamic principles
- No distinct head or tail as for most flying objects
- Many technical disciplines involved
- Different couplings between disciplines

Decaying satellites are usually SC without any aerodynamic design input. This means the code must have the capability to treat Spacecraft of general and complex shape without aerodynamic head or tail.
A second demand resulted from the coupling of analysis methods covering 5 different disciplines as shown in Fig.1.
There exists in addition a strong mutual influence between analysis methods and the spacecraft modelisation. The physical depth of the analysis methods determines the effort and complexity of the SC modelisation. Another extreme important point is, that during the destruction process the geometry and physical data of the SC are continuously changing. This requires the capability of a self adjusting model.

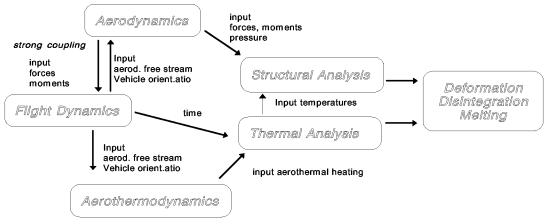

The coupling and dependence between the different physical disciplines for disintigration prediction

Fig.1 The coupling between different disciplines for disintegration prediction

2. The space craft modelling with SCARAB

- The modelling consist of
- Geometric modelling
- Material data base
- Physical modelling

2.1 Geometric modelling.

The geometry module provides panellized geometric primitives, Fig. 2, whose size, shape and position can be parametrically adjusted. This allows reconstruct the external and internal components of the spacecraft. According to specified wall thickness the surface elements are transformed to volume elements. Complex shapes can be generated by combination of these shapes

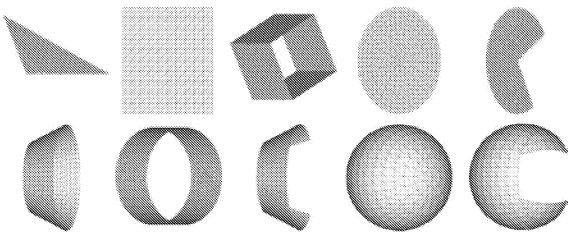

Fig.2 Set of geometric primitives available in SCARAB

2.2 The material data base

SCARAB is equipped with material data base in which most of the common materials used for SC are included. The data base contains for each material 20 physical

Proceedings of the Fifth European Symposium on Aerothermodynamics for Space Vehicles, 8-11 November 2005, Cologne, Germany (ESA SP-563, February 2005)

properties. Properties like heat capacity, conductivity, ultimate tensile stress and emission coefficient are modelled with temperature dependence up to the melting point. SCARAB version 2 [4] includes orthotropic and multilayerd materials. A further extension in work is a full '3 phase material data base' covering solid. liquid and gaseous phase including the phase transition.
A main problem is still the modelling of carbon fibre reinforced plastics (CFRP)
During the physical modelling materials are appointed to each component and mass, centre of mass, and moments of inertia are determined.
The physical model provides the basis for all analysis modules, and it therefore should match the physical data of the real spacecraft. In order to achieve this, the modelling must follow the synthetic structure of the spacecraft, starting with the top level (level 1) structure, and then modelling the subsystems (level 2 and lower).

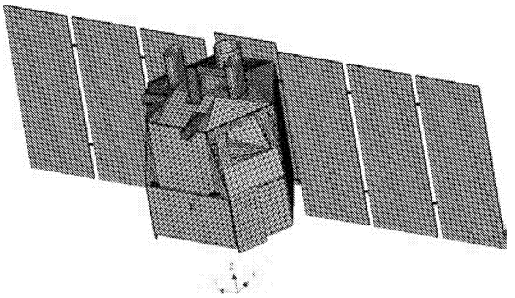

Fig.3 Beppo Sax Satellite modelled with SCARAB

3. The analysis modules of SCARAB

The analysis modules of SCARAB are

- Flight dynamics analysis with 6 degree of freedom
- Aerodynamic and aero-heating analysis
- Thermal analysis
- Structural analysis
- Destruction analysis by local melting or fracture.
- Fragment tracking

Between these modules the SC-model all necessary communication chains are established. Analysis results along the trajectory are stored in history files.
The re-entry analysis can be organized in chained loops, which allow for each time step of flight dynamics analysis a new aerodynamic or aero-thermal analysis.

3.1 The flight dynamics analysis

The trajectory and attitude motion of the SC and of fragments during melting phase is determined is determined by numerical integration of the 6 dof equations of motion describing change of momentum due to external force and torque.

$$\frac{d}{dt}(m\vec{V}) = \vec{F}_{ext}\,; \quad \frac{d}{dt}(mI\vec{\omega}) = \vec{M}_{ext}$$

External forces and moments are due to gravity (earth, sun, moon) and due aerodynamic pressure and shear stress. Integration is performed with Runge Kutta method with fixed or variable step size.
After the finishing of the melting phase (Ma <6) the flight dynamics of fragments is tracked with a 3dof method till ground impact.

3.2 The aerodynamic and aero-heating analysis

The aerodynamics is based on local panel methods, this means that for each elementary surface panel pressure, shear stress and heat transfer rates are calculated. The integration over all surface elements gives then the integral aerodynamic forces and moments.

$$\vec{F}aero = q_\infty \int_S (c_p\vec{n} + c_\tau\vec{t})dS$$

$$\vec{M}aero = q_\infty \int_S (\vec{r}\times c_p\vec{n} + \vec{r}\times c_\tau\vec{t})dS$$

The panel aerodynamics is applied in the hypersonic regime (Ma >5) and it distinguishes between free molecular flow, rarefied–transitional flow, continuum flow

Free molecular flow regime
Using Schaaf-Chambre accomodation coefficients [5] the local pressure, shear stress coefficients are given by

$$.c_{pFM} = \frac{\sigma_N}{\sqrt{\pi}S_\infty^2}\left[\frac{2-\sigma_N}{\sigma_N}\Pi(S_n) + \frac{1}{2}\sqrt{\frac{T_w}{T_\infty}}\chi(S_n)\right]$$

$$c_{\tau FM} = \frac{\sigma_\tau}{\sqrt{\pi}S_\infty}\sin(\theta)\chi(S_n)$$

With S the molecular speed ratio and $Sn = Scos(\theta)$ its normal component to an inclined surface element.
Π and χ are functions of S_n

Hypersonic continuum flow regime
In continuum flow a modified Newtonian method is applied for surface pressure:
Wetted surface ($\theta < \pi/2$)

$$c_{PC} = k_{N1}(\kappa, Ma, \theta)\cos^2(\theta) + k_{N2}(\kappa, Ma, \theta)$$

Skin friction is set to zero, which is acceptable for blunt bodies.

$$c_{\tau C} = 0$$

Rarefied transitional flow regime
The local aerodynamic coefficients are calculated with local bridging functions f_P and f_τ , which have been validated against experimental data [6].
The general formulation is as follows

$$c_p = c_{pC} + (c_{pFM} - c_{pC})f_P(Kn_{\infty,0})$$

$$c_\tau = c_{\tau C} + (c_{\tau FM} - c_{\tau C})f_\tau(Kn_{\infty,0})$$

$Kn_{,\infty 0}$ is a Knudsen number based on free stream density and stagnation point temperature and viscosity.

Free molecular heating
The local free molelucar heat transfer Stanton number St_{FM} is calculated with the standard formulation equivalent to pressure and shear stress.

Continuum heating
Continuum heating is related to the stagnation point Reynoldsnumber and to the local inclination θ of the surface element

$$St_C = \frac{2.1}{\mathrm{Re}_{\infty,0}}(0.1 + 0.9\cos(\theta))$$

$\mathrm{Re}_{\infty,0}$ is defined as follows

$$\mathrm{Re}_{\infty,0} = \frac{\rho_\infty V_\infty r_N}{\mu(T_0)}$$

With r_N the effective nose radius of the object and $\mu(T_0)$ the stagnation point viscosity. We use a power law viscosity dependence on temperature T with

$\mu(T_0)/\mu(T_\infty) = (T_0/T_\infty)^\omega$ and $\omega = 0.72$.

For the stagnation point the above formula reduces then to an equivalent expression as Detra, Kemp Ridell [7]

Rarefied transitional heating
For the transition regime during re-entry the following bridging formula is used:

$$St = \frac{St_C}{\sqrt{1 + (St_C/St_{FM})^2}}$$

This bridging formula was originally derived by Legge [8] and validated against many experiments.

Low speed aerodynamics (0< Ma< 5)
In this regime melting and fragmentation is finished and therefore only survival fragments of the original SC have to be treated.
By inspection of projected area of these fragments SCARAB [xx] distinguishes between bluff and long slender bodies. Then a bridging method with anchoring points at Ma = 0, 1 and 5 is used to determine Drag and Lift coefficients as function of Mach number. The following table outlines this.

Table 1 Aerodynamics between Ma = 0 and 5q

Body type	Aero –coefficents	Method
Bluff	only drag	Bridging Ma =0,1,5
Slender	drag and lift	Cross flow method
Rotating	only drag	Integral for period

Special features of the aerodynamic methods

a. Universal shadowing analysis
The shadow analysis applies to external and internal surface elements.
a. External aerodynamic shadow for Ma >>1
The local panel methods can only be applied to surface elements not shadowed by other parts of the vehicle.

b. Shadowed internal surface elements.
Internal surface elements have to be excluded from analysis. They have however selectively to be included in the aerodynamic analysis in case a hole is burned into the external surface and internal parts become thus exposed to the flow

SCARAB has therefore been equipped with a shadow analysis method which continously checks all internal and external surface elements if they are aerodynamically active or not.

b. Streamline dependent skin friction and heating method.
This requires the detection of stagnation points, determination of the effective radius of curvature at stagnation point and the determination of streamline length up to a selected surface element. For our SCARAB 3 the necessary methods have been developed and coded [xx]. Practical testing showed that this approach is only feasible for well defined shapes as re-re-entry capsules or winged vehicles.

3.3 Thermal analysis.

The adopted thermal model relies on SC geometry consisting of shell type elements.
The heat flow balance for a single panel is as follows

$$q'_{pan} = q'_{aero} + q'_{rad} + q'_{cond}$$

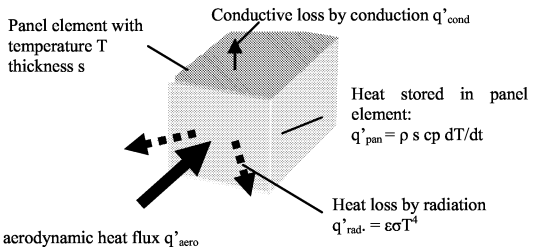

Heat flow balance for wall surface panel

Fig. 3 Heat flow balance for surface panel

Thin panel heating
If heat conductivity of panel material is large or the panel thicknes s is extremely thin, temperature gradients in the panel can be neglected and we get for the panel heating rate

$$q'_{pan} = \rho c_P s dT/dt \quad \text{for} \quad T > T_{melt}$$

itf the melting point tmelt is reached the panel temperature will stay at Tmelt and the heat flux into the panel will melt the panel wall from the outer surface. Thus the solid wall thickness d will start to decrease.

$$q'_{pan} = \rho h_{melt} ds_m/dt \quad \text{for} \quad T = Tmelt$$

where s_m= denotes thickness of melt layer.
When s_m = s the panel is completely molten.
In SCARAB we assume that after panel melting the panel liquid mass is blown away from the vehicle.

Thick panel heating
If the thermal relaxation time τ of the panel exceeds the characteristic time for external heat flux changes then the panel is divided into a Number of N layers (Thermal nodes) with equal thickness $s_{node} = s_{pan}/N$ and the heat flux from node I to j is calculated by

$$q'_{i\to j} = \lambda(T_i - T_j)/s_{node} \text{ for } \tau = s^2 \rho c_P / \lambda > \tau_{aero}$$

Melting is then monitored on layer level. This allows treatment of solid bodies with low heat conductivity.

3.4 Structural analysis

The analysis method used in the SCARAB 1.5 version is an engineering method and restricted to stress and fracture analysis in predefined cut planes. Elementary elements are joints and sections through one or more joints which are positioned within a cut plane.
SCARAB determines then the differential loads resulting from aerodynamic forces and inertia forces and conducts a stress analysis for the sections at cut position.

$$\sigma = \frac{Fx}{A} + \frac{M_y z}{J_y} + \frac{M_z y}{J_z}; \tau = \frac{M_x \rho}{J_\rho}$$

Fracture condition is given by

$$\sigma_{eq} = \sqrt{\sigma^2 + 3\tau^2} \geq \sigma_{ult}(T)$$

In the stress analysis the reduction of the ultimate material stress with element temperature at the cut plane is considered.
In the SCARAB 2 version in addition a finite element analysis method for thin shells has been implemented.

3.5 Interaction between analysis modules.

During melting of panels the modelled SC looses mass, internal surfaces become exposed to the flow and the geometry of the SC changes.
All these changes are communicated between the different modules. Thus SCARAB considers during the melting process the following effects [9]:

- Change of mass, shift of CM, change of moment of inertia matrix
- Change of active aerodynamic surface elements.
- Exposure of internal surfaces to flow.

4 SCARAB applications

Before direct application benchmark calculations between the NASA ORSAT code [10] and SCARAB have been conducted [11]. Within this study the demise altitude of hollow spheres was comparatively compared.
Up to now SCARAB has been used to analyse the destructive re-entry of the following SC:ATV, ARIANE 5 cryogenic main stage EPC and upper stage VEB/EPC, BeppoSAX,, TERRASAR-X [12];[13],[14],[15].
In the following we demonstrate the SCARAB capabilities on the example VEB /EPS

4.1 The SCARAB EPS/VEB Model

The Ariane 5 upper stage consists of the Vehicle Equipment Bay (VEB), the Etage a Propergol Stockable (EPS), and the Separation and Distancing Module SDM. The SCARAB model of the complete VEB/EPS assembly [XX] is shown in

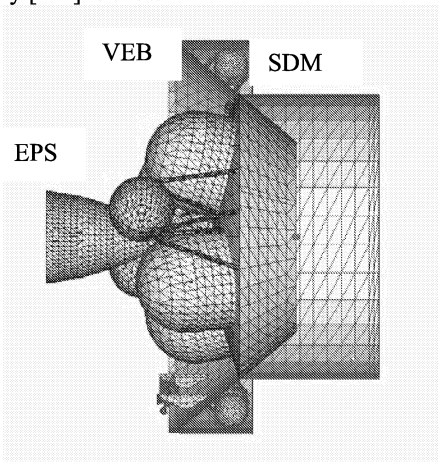

Fig. 4. Geometry EPS/VEB model

The complete VEB/EPS/SDM group was modelled with 229 basic geometric elements having 65372 surface and 26817 volume panels.

Vehicle Equipment Bay, VEB
The VEB consists of the structure, two thruster brackets with four 400N hydrazine thrusters each; 6 propellant tanks and an electrical equipment ring. A simplified mass budget comparison is shown in the following table. Fig. 5 shows the VEB from bottom and top direction.

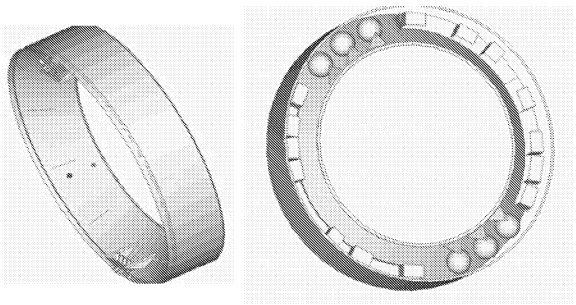

Fig. 5 VEB Scarab model; bottom and top view

The EPS
The EPS was modelled with 90 basic geometric elements. The dry EPS mass of 1237 kg is modelled by SCARAB with 1233.5 kg. The EPS structure supports two MMH and two N2O4 tanks. The engine is mounted with cardan and actuator

struts. The EPS contains in its tanks unused propellant of 505 kg. This propellant was modelled as liquid sheet covering the inside of the N204 and MMH tanks.

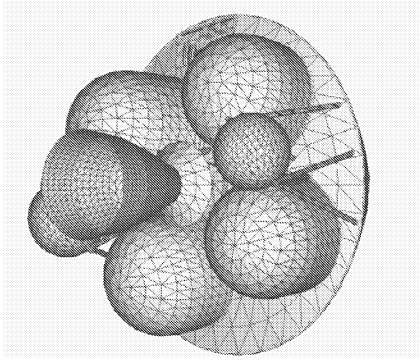

Fig.6 The EPS Scarab model view to bottom

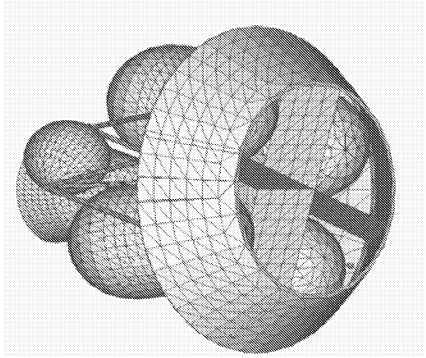

Fig. 7 EPS Scarab model View from top

The Separation Distancing Module SDM
The SDM is mounted on top of the VEB/EPS and is the interface to the ATV. Only parts remaining on EPS after ATV separation have been modelled. These parts are separation distancing cylinder and separation system with clamp rings.
On total the VEB/EPS/SDM SCARAB model consisted of 229 basic elements with 65372 surface panels.
Table 2 Mass, CG and inertia matrix VEB/EPS/ACY

		CG Locations			Moment of inertia		
	Mass, kg	Xcg m	Ycg m	Zcg m	Ixx kgm^2	Iyy kgm^2	Izz kgm^2
VEB	1078,3	0,951	0,000	-0,007	7335	4380	3201
EPS	1737,2	-1,264	0,015	-0,007	2899	2552	2151.
ACY	239,8	1,114	0,000	0,000	911	564	563.
Total	3055,3	-1,131	0,011	0,066	11148	8058	6479

4.2. Initial Conditions for re-entry analysis

The initial conditions were specified as follows:
Initial epoch: H0 + 5204s
Position and velocity in Earth-fixed coordinates:
X = -361.467 km, Y = -6305.72 km, Z = -2168.833 km
V_x = 4324.32 m/s, V_y = -2076.69 m/s, V_z = 5319.96 m/s
Attitude and rotational state in body-fixed coordinates:
$\varphi = 0°$, $\theta = 0°$, $\psi = 0°$; $\omega_x = 60°/s$, $\omega_y = 8°/s$, $\omega_z = 0°/s$
Geodetic coordinates: h = 302 km; longitude -93.28°, latitude -19.06°.

4.3 Re-entry and attitude motion

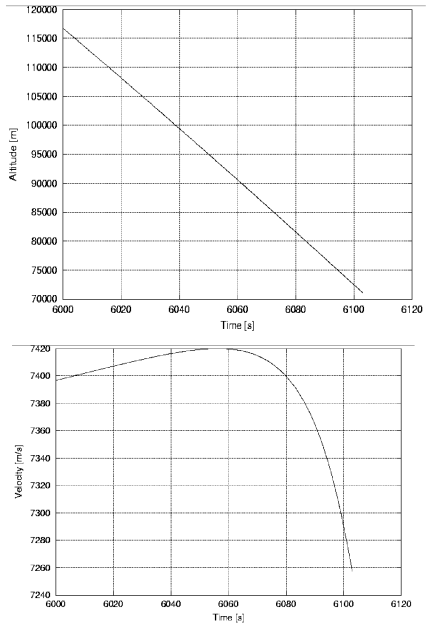

Fig. 8 Altitude and velocity versus time

Fig 8 shows altitude and velocity versus time.Capture in the atmosphere occurs after = 6060 s at 100 km altitude This is also observed in the change of angular motion shown in Fig. 9.

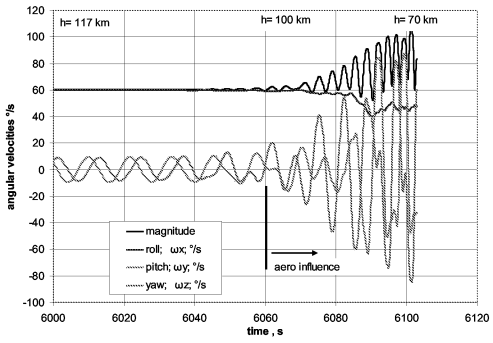

Fig.9 Angular velocities till first break up.

Drag and lift coefficients during re-entry are shown in Fig. 10 and 11.

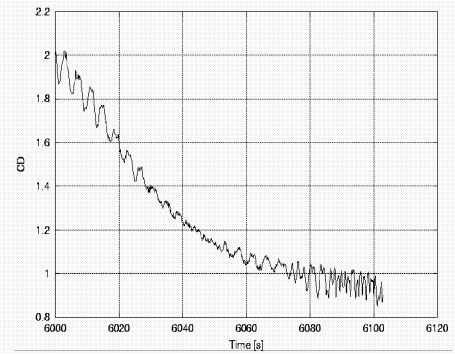

Fig.10 Drag coefficient C_D as function of time

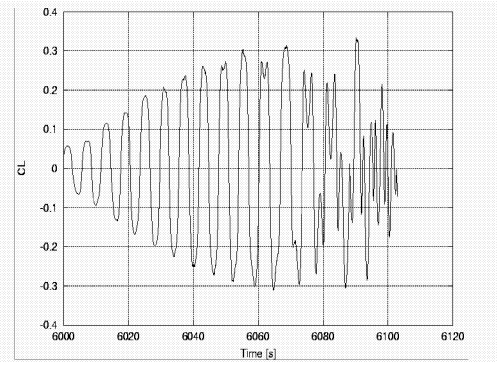

Fig. 11Lift coefficient C_L as function of time

The thermal destruction starts at 82 km and the first thermal fragmentation occurs about 18 s later at an altitude of 71.1 km as can be seen from Fig.12.

The mass history of the main fragment is shown in Fig. 13. We observe two classes of mass reductions namely by melting and by fragmentation.

A summary of all fragmentation events is shown in Fig. 14. At first the thermal destruction of the SDM occurs, which is derictly exposed to the flow. After a longer time intervall the thermal destruction of the VEB takes place and finally EPS is destructed by mechanical loads. Fig. 15 shows VEB/EPS during destruction of the SDM.

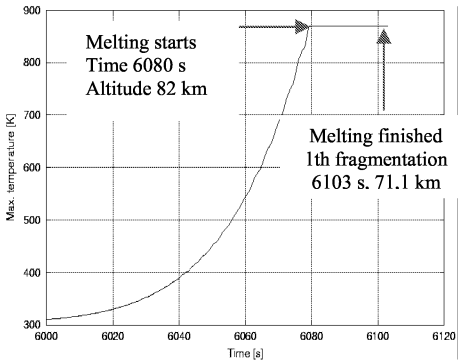

Fig.12 Thermal history of element

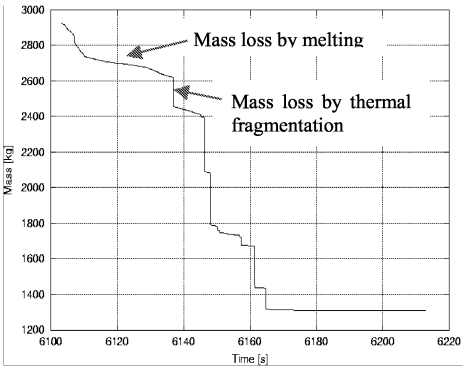

Fig. 13 Mass history of main Fragment

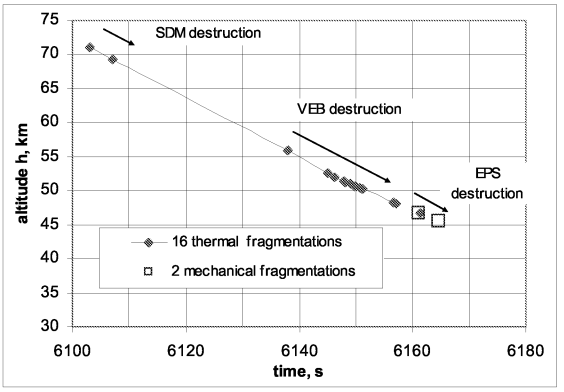

Fig. 14 Fragmentation events in altitude time chart

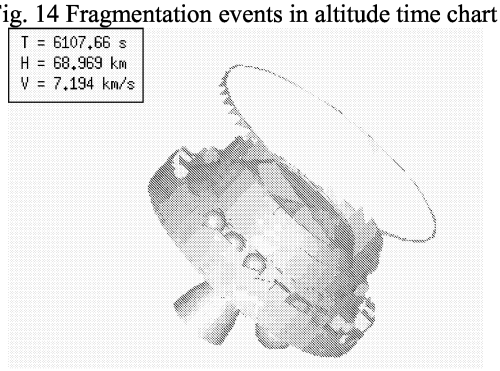

Fig.15 Destruction of the SDM duringre-entry

From the EPS/VEB upper stage 17 fragments will reach the ground.

5. Conclusions

A short description of the principal methods used in SCARAB has been given. A truly multidisciplinary software could be realised by a consistent development of the modules covering the different disciplines

This required too abandon for the aerodynamic analysis codes which need flow field volume grids. SCARAB analysis methods are based on panelised surfaces with artificial volume panels for the solid structure.

This allows to continuously reconstruct the actual SC configuration during the destruction process and to analyse fragments till complete demise or ground impact.

Literature

[1] B. Fritsche, H. Klinkrad, A. Kashkovsky, E. Grinberg,. Spacecraft Disintegration During Uncontrolled Atmospheric Entry. Acta Astronautica 47, Elsevier Science Ltd, London, U.K., pp. 513-522, 2000.

[2] B. Fritsche B. et alea, Spacecraft disintegration during uncontrolled atmospheric Re-entry.
Executive Summary, ESOC Contract No. 11427 /95/D/IM; Lindau , Germany 1997

[3] B. Fritsche, H. Klinkrad, A. Kashkovsky, and E. Grinberg., Application of SCARAB to Destructive Satellite Re-Entries. IAA-99-IAA.6.5.08, 51st IAF Congress, Rio de Janeiro, Brazil, 2000.

[4] B. Fritsche et alea,
Uncontrolled Re-Entry of Risk Objects
Final Report, ESOC Contract No. 13946/99/D/CS
HTG Lindau , Germany , 2002

[5] N. M. Kogan; Rerfied Gas Dynamics
Plenum Press, New York, 1969

[6] G. Koppenwallner , M. Ivanov; D. Johannsmeir; A. Kaskovsky; Free Molecular and Transitional Aerodynamics of Spacecraft; ESOC Contract 10032/92/D/IM, HTG Germany 1994

[7] R.W. Detra,. N.H. Kemp., F. R. Ridell., Addendum to Heat Transfer to Satellite Vehicles Reentering the Atmosphere
Jet Propulsion Vol.27 No.12 pp. 1256-1257, 1957

[8] H. Legge Hypersonic approximations for heat transfer and shear stress applied to continuum and rarefied plume impingement
DFVLR- IB 222-87 A23; 1987

[9] T. Lips, B. Fritsche, G. Koppenwallner, and H. Klinkrad. Spacecraft Destruction During Re-entry – Latest Results and Development of the SCARAB Software System. Advances in space Research 34, pp 1055-1060, Elsevier 2004.

[10] W.C. Rochelle ,B.S. Kirk, B.C. King
Users Guide for Object Reentry Survival Analysis Tool (ORSAT)-Version 5, Vol. 1, JSC-28742; NASA, Lyndon B. Johnson Space Center, 1999

[11] Klinkrad H;. Fritsche B.
Thermal destruction of hollow spheres during atmospheric entry.
Test results computed with the SCARAB S/W system
16th IADC Meeting Toulouse 1998

[12] B. Fritsche, G. Koppenwallner, and T. Lips. Reentry Analysis for the ATV with SCARAB. Final Report. ESA Contract No. 13946/99/D/CS, HTG - Hyperschall Technologie Göttingen, Katlenburg-Lindau, Germany, 2001.

[13] G. Koppenwallner and B. Fritsche. Re-entry Analysis of Ariane 5 EPC and Ariane 5 EPS/VEB, Technical Report Compilation. ESA Contract No. 15401/01/F/IZ, HTG - Hyperschall Technologie Göttingen, Katlenburg-Lindau, Germany, 2003.

[14] C. Portelli, L. Salotti, L. Anselmo, T. Lips, and A. Tramutola. BeppoSAX Equatorial Uncontrolled Re-entry. PEDAS1-B1.4-0027-02, Presentation at the World Space Conference 2002, Houston, USA, 2002

[15] T. Lips, B. Fritsche, G. Koppenwallner, A. Zaglauer, and R. Wolters. Re-Entry Analysis of TerraSAR-X with SCARAB. IAC-03-IAA.5.4.02, 54th IAF Congress, Bremen, Germany, 2003.